Fuel 325 (2022) 124940

Contents lists available at ScienceDirect

Fuel

journal homepage: www.elsevier.com/locate/fuel

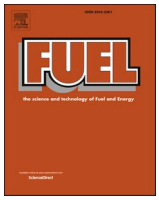

Full Length Article

Comparative study on ignition characteristics of n-propylbenzene, 1,3,5-trimethylbenzene and 1,2,4-trimethylbenzene behind reflected shock waves

Jinhu Liang [a,*], Fei Li [a], Shutong Cao [a], Xiaoliang Li [a], Ming-Xu Jia [b], Quan-De Wang [b,*]

[a] School of Environmental and Safety Engineering, North University of China, Taiyuan 030051, People's Republic of China
[b] Jiangsu Key Laboratory of Coal-Based Greenhouse Gas Control and Utilization, Carbon Neutrality Institute and School of Chemical Engineering, China University of Mining and Technology, Xuzhou 221008, People's Republic of China

ARTICLE INFO

Keywords:
Trimethylbenzene
Propylbenzene
Shock tube
Ignition delay time
Chemical kinetic modeling

ABSTRACT

Alkyl aromatics comprise a significant portion of real fuels. Among various alkyl aromatics, the C_9H_{12} aromatic fuels including n-propylbenzene and trimethylbenzenes are representative alkyl aromatics, which are widely detected in real fuels, and they are widely employed as surrogate compounds in modeling real fuels. Thus, the combustion kinetic study of C_9H_{12} fuels is necessary and urgent for fuel combustion. In this work, comparative experimental and kinetic modeling study of the high-temperature ignition of three C_9H_{12} fuels is performed. New ignition delay time (IDT) measurements are carried out in a high-pressure shock tube (HPST) for 1,2,4-trimethylbenzene and 1,3,5-trimethylbenzene. The studied pressure is 2, 5 and 10 bar, the equivalence ratios are 0.5, 1.0 and 2.0, and the temperature range is from 1090 K to 1600 K for IDT in HPST. The experimental results are simulated using an updated detailed kinetic mechanism. Reaction path analysis and sensitivity analysis are performed to provide insight into the chemical kinetics controlling the ignition of the three C_9H_{12} fuels. The present experimental data set and kinetic model results should be valuable to improve our understanding of the combustion chemistry of alkyl aromatics and to offer practical guidance for the surrogate model development of real fuels.

1. Introduction

Alkyl aromatic compounds represent an important class of ingredients in real fuels, i.e., gasoline, diesel, and jet fuels [1–3]. Thus, a better understanding of the combustion characteristics and combustion chemical kinetics of real fuels requires a fundamental understanding of combustion chemistry of alkyl aromatics. Besides as energy sources in real fuels, these compounds can form Polycyclic Aromatic Hydrocarbons (PAHs) and soot easily during combustion processes [4], which has negative effect on human health and environment protection. Therefore, during the past decades, various experimental measurements and kinetic modeling studies have been performed to obtain combustion properties of alkyl aromatics. Among various alkyl aromatics, C_9H_{12} hydrocarbons including propylbenzenes and trimethylbenzenes are representative alkyl aromatic compounds. They are widely existed in real diesel and aviation fuels, and are usually employed as representative compound in the development of surrogate model of real fuels [3,5–10]. Hence, the combustion kinetic study of C_9H_{12} hydrocarbons receives significant attentions in combustion community.

Specifically, the C_9H_{12} aromatic hydrocarbons contain single side-chain alkyl aromatics, i.e., n-propylbenzene (NPB) and i-propylbenzene (IPB) and multiple side-chain alkyl aromatics, including 1,2,4-trimethylbenzene (T124MB), 1,3,5-trimethylbenzene (T135MB), 1-ethyl-2-methylbenzene, 1-ethyl-3-methylbenzene, and 1-ethyl-4-methylbenzene. Among these C_9H_{12} isomers, NPB has been investigated extensively in the literature. Various experimental facilities together with kinetic modeling have been performed to investigate the species profiles [11,12], laminar flame speeds [13], ignition delay times (IDT) [14], and soot tendency [4] of NPB. The research results provide a good foundation for the use of NPB as a model compound in surrogate model of real fuels [3,7]. In contrast to NPB, the oxidation and combustion of IPB receives less attention. Only some experimental and kinetic modeling studies on the pyrolysis process and soot tendency has been reported [15,16].

* Corresponding authors.
E-mail addresses: jhliang@nuc.edu.cn (J. Liang), quandewang@cumt.edu.cn (Q.-D. Wang).

https://doi.org/10.1016/j.fuel.2022.124940
Received 25 April 2022; Received in revised form 14 June 2022; Accepted 16 June 2022
Available online 23 June 2022

Due to the great interest in the usage of T124MB and T135MB as a substitution compound in surrogate model development, the combustion kinetic of T124MB and T135MB has been extensively studied recent years. The combustion characteristics including ignition, laminar flame speeds, species profiles were extensively measured covering a wide range of combustion conditions. For example, the low temperature ignition characteristics of T124MB and T135MB were studied [17,18] using rapid compression machine (RCM), while the high-temperature IDTs of T135MB have been measured in shock tube (ST) by Rao et al. [19]. Laminar flame speeds were also measured for the two compounds counter-flow flame facility [20,21]. Other related previous studies on the C_9H_{12} fuels have been also summarized by Liu et al. [22], and in their work, a comparative study on the oxidation of NPB, T124MB and T135MB in a jet-stirred reactor with temperature range from 700 to 1100 K has been performed. However, to the best of our knowledge, no high-temperature IDTs has been reported for T124MB. Thus, a detailed comparison of the high-temperature ignition characteristics of the three typical C_9H_{12} aromatic hydrocarbons is still not implemented.

Based on the above considerations, this work reports a comparative study on the ignition characteristics of NPB, T135MB and T124MB using ST measured IDTs. New IDTs measurements are carried out in a high-pressure shock tube (HPST) for T124MB and T135MB. An updated detailed kinetic mechanism has been developed and used for kinetic modeling studies. Reaction path analysis and sensitivity analysis have been carried out to demonstrate the structural effect on the ignition characteristics of the three C_9H_{12} aromatic fuels.

2. Experimental methods

In this work, IDTs are measured in a high-pressure shock tube (HPST) at North University of China (NUC). The facility has been detailed in previous studies [3,23], and thus are briefly described here. The HPST is composed of a 3.0 m driver section, a 6.8 m driven section, and a 0.3 m double diaphragm section connecting the driven and driver sections with an inner diameter of 100 mm. The incident shock velocity is measured using five PCB 113B26 piezoelectric pressure transducers mounted on the sidewall of the driven section. A PCB 113B26 piezoelectric pressure transducer mounted 20 mm away from the endwall of the driven section is used to record the pressure–time profiles. All pressure and emission signals are recorded using two digital TiePie Handyscope HS4 oscilloscopes. The reflected wave pressure and temperature are determined using the one-dimensional normal shock relations by the Gaseq program [24]. The pressures and emissions of OH* at 306.5 nm behind reflected shock waves are recorded after bursting of the diaphragms. IDT is defined as the time interval between the arrival of the reflected shock wave and the onset of OH* emission at the sidewall observation location or the maximum rate of rise of the pressure signal. The onset of ignition is observed in the OH* emission history defined by linearly extrapolating the maximum slope to the baseline of the emission trace. Fig. 1 shows an example of the pressure and OH* emission signal traces for T124MB in air at 1181 K and 9.93 bar with equivalence ratio of 1.0. The shock attenuation range during the experiments is within 0.25%-0.86%, and it is quite well. During all the experiments, the IDTs measured by the onset of OH* emission and the maximum rate of rise of the pressure signal are almost the same.

All mixtures are prepared in stainless steel mixture tanks according to the Dalton's law of partial pressure, and the prepared mixture is maintained at least twelve hours before experiments to ensure the complete vaporization and homogeneity. The purities of oxygen and nitrogen used in this experiment are larger than 99.5%. The purity of Ar is 99.99%. Helium is used as driven gas in HPST, and the purity is also 99.99%. A heating system with seven thermocouples placed along the mixing tank, shock tube and the sampling tube is used to maintain the experimental system with a temperature of 398 K to avoid adsorption of the liquid fuel. Table 1 lists the HPST experimental conditions in this work. For the uncertainty in the measured IDTs behind reflected shock

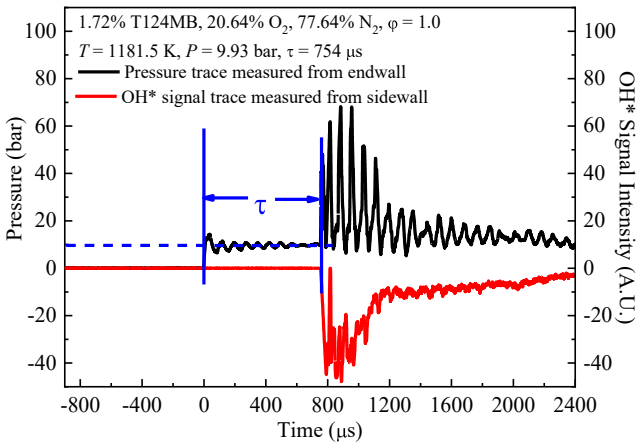

Fig. 1. Typical pressure and OH* emission signal traces for T124MB measured in this work (The values of OH* emission signals are shown in their negative values to differ with the pressure trace).

Table 1
HPST experimental conditions in this work.

Fuel	φ	x_{Fuel} (mol%)	x_{O2} (mol %)	x_{N2} (mol %)	Avg. P_5 (bar)	T_5 range (K)
T124MB	0.5	0.867	20.818	78.315	2.0, 5.0, 10.0	1150–1550
	1.0	1.72	20.639	77.641	2.0, 5.0, 10.0	1140–1560
	2.0	3.382	20.290	76.328	2.0, 5.0, 10.0	1210–1600
T135MB	0.5	0.867	20.818	78.315	2.0	1290–1550
	1.0	1.72	20.639	77.641	2.0	1320–1540
	2.0	3.382	20.290	76.328	2.0	1280–1520
NPB	0.5	0.867	20.818	78.315	2.0, 5.0	1110–1460
	1.0	1.72	20.639	77.641	2.0, 5.0	1090–1440
	2.0	3.382	20.290	76.328	2.0, 5.0	1110–1440

tube, Petersen et al. [25] performed detailed analysis, and the uncertainty is changing by changing in the compressed temperature and pressure, and equivalence ratio [25,26]. Thus, it is not a constant parameter during the different experimental conditions. According to detailed literature analysis [25–27], and also the conditions studied here, the largest uncertainty of temperature behind the reflected shock wave is estimated to be ± 20 K, and the averaged uncertainty for the measured IDTs can be controlled within ± 20% [3,23], and are generally consist with the other related facilities [26,28–30].

3. Kinetic model development

To develop a unified detailed kinetic mechanism for the three studied hydrocarbons, the recently developed skeletal NUIGMECH1.1 mechanism has been employed as the base model because this mechanism has been developed systematically and hierarchically by re-evaluating the kinetics and thermochemistry of C_0-C_4 base chemistry based on recent ab-initio studies and experimental diagnostics and has been extensively validated for the core C_0-C_4 fuels [23,31–35]. Although various detailed kinetic mechanisms have been developed for NPB, T124MB and T135MB, they were mainly used for specific targets. For example, the JetSurF 2.0 mechanism [36] was developed mainly for benzene, toluene, ethyl benzene, and n-propylbenzene, and branched alkyl aromatics were not considered. The Liu mechanism showed [22] acceptable performance in the prediction of jet-stirred reactor experimental results, but it is shown that the mechanism is hard to get convergence results during ignition simulations. After an initial assessment of literature mechanisms, it is shown that the detailed kinetic mechanism developed by Kukkadapu et al. [37] for C_7-C_{11} methylated aromatics including sub-

mechanisms of T124MB and T135MB exhibits relatively good performance for ignition simulations. In addition, it is worth noting that the Kukkadapu mechanism was developed based on the similar reaction classes from earlier mechanism for alkyl-benzenes published by Mehl et al. [13] for ethylbenzene, NPB and n-butylbenzenes. The old version of NUIGMECH1.1 mechanism, i.e., AramcoMech 2.0 was used to describe the C_0-C_4 chemistry. Thus, to keep consistence and keep pace of the base mechanism development, the sub-mechanisms of NPB, T124MB, and T135MB have been coupled with the skeletal NUIGMECH1.1 mechanism for the present IDT simulations. However, it is shown that the present mechanism generally exhibits very similar performance compared with that using the Kukkadapu and Mehl mechanisms for the studied fuels, indicating the updated base chemistry of C_0-C_4 shows little effect of the studied alkyl aromatics fuels. The detailed mechanism is composed of 1105 species and 6219 reactions. Kinetic modeling for ignition is performed by using Cantera software [38] assuming a closed homogeneous batch reactor at constant volume, which has been confirmed to be adequate for kinetic simulations of shock tube IDTs from short test times (which occur at high-temperatures) [39–41].

4. Results and discussion

4.1. IDT characteristics of the three C_9H_{12} fuels

The measured IDT results in the present work together with literature data for the oxidation of the three C_9H_{12} fuels are shown in Fig. 2, while kinetic modeling results are shown in Fig. 3. From Fig. 2, it is demonstrated that the IDTs of NPB tend to be faster than that of T135MB and T124MB for a given combustion conditions, i.e., temperature, pressure, and equivalence ratio. At equivalence ratios of 0.5 and 1.0, the IDTs of T124MB are slightly faster than that of T123MB, indicating T124MB exhibits more reactivity than T135MB at these conditions. However, it is shown that as the equivalence ratios increase, the IDTs between T124MB and T135MB for a given combustion condition are very close to each other and are nearly indistinguishable. To sum up, the overall reactivity of the three C_9H_{12} fuels exhibit the following tendency with NPB > T124MB > T135MB, which is also in good agreement with previous studies from Jet-stirred reactor studies [22]. The equivalence ratio shows significant effect specifically on the relative reactivity of T124MB and T135MB.

From Fig. 3, the detailed kinetic modeling results for the three fuels under the studied combustion conditions are in good agreement with experimental results. The pressure, temperature, and equivalence ratio effects on the IDTs are well reflected using the detailed mechanism. For the three C_9H_{12} fuels, it can be seen that the pressure, temperature, and equivalence ratio effects on the IDTs are similar. Specifically, the IDTs decrease as the pressure increases, indicating the reactivity increases as pressure increases. However, the pressure effect on the IDTs for three fuels are different as shown from the narrow gaps between different pressure conditions. The IDTs of the three fuels exhibit Arrhenius behaviors as a function of temperature. Although the equivalence ratio shows some effect on the IDTs of the three fuels, it is found that the IDTs are only very slightly affected by the equivalence ratio as shown in Fig. 4 for the three fuels at 2, 5 and 10 bar with different equivalence ratios. During the studied conditions, no obvious negative temperature coefficient region is observed for all the three fuels. Finally, it is shown that the data all illustrate the same Arrhenius behavior with apparent identical pressure and mixture dependencies for all fuels, thus, the IDTs are correlated to a general Arrhenius dependence expression using the following formulas [44], i.e., $\tau_{ign} = A[Fuel]^a[O_2]^b \exp\left(\frac{E_a}{RT}\right)$ and $\tau_{ign} = A' P^{\alpha} \varphi^{\beta} \exp\left(\frac{E_a}{RT}\right)$, where τ_{ign} is IDTs in ms, A is a pre-factor, E_a represents the global activation energy in J mol^{-1}, T is the temperature in K, P is the pressure in bar, φ is the equivalence ratio, and $R = 8.314$ J mol^{-1} K^{-1}, is

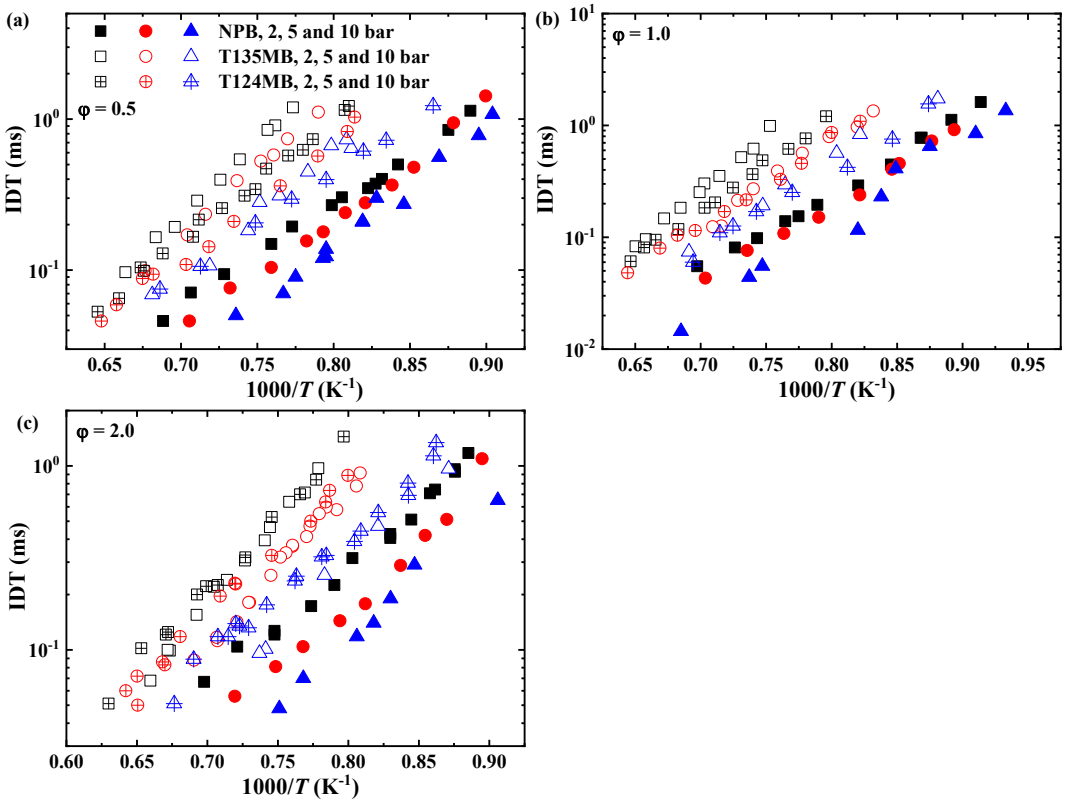

Fig. 2. Comparisons of IDTs for NPB, T135MB, and T124MB at different conditions. The IDTs of NPB at 10 bar with equivalence ratios of 0.48, 0.96 and 1.92 are taken from the results by Darcy et al. [42], while the IDTs of T135MB at 5 and 10 bar with equivalence ratios of 0.5, 1.0 and 2.0 are measured by Rao et al. [19] and Diévart et al. [43].

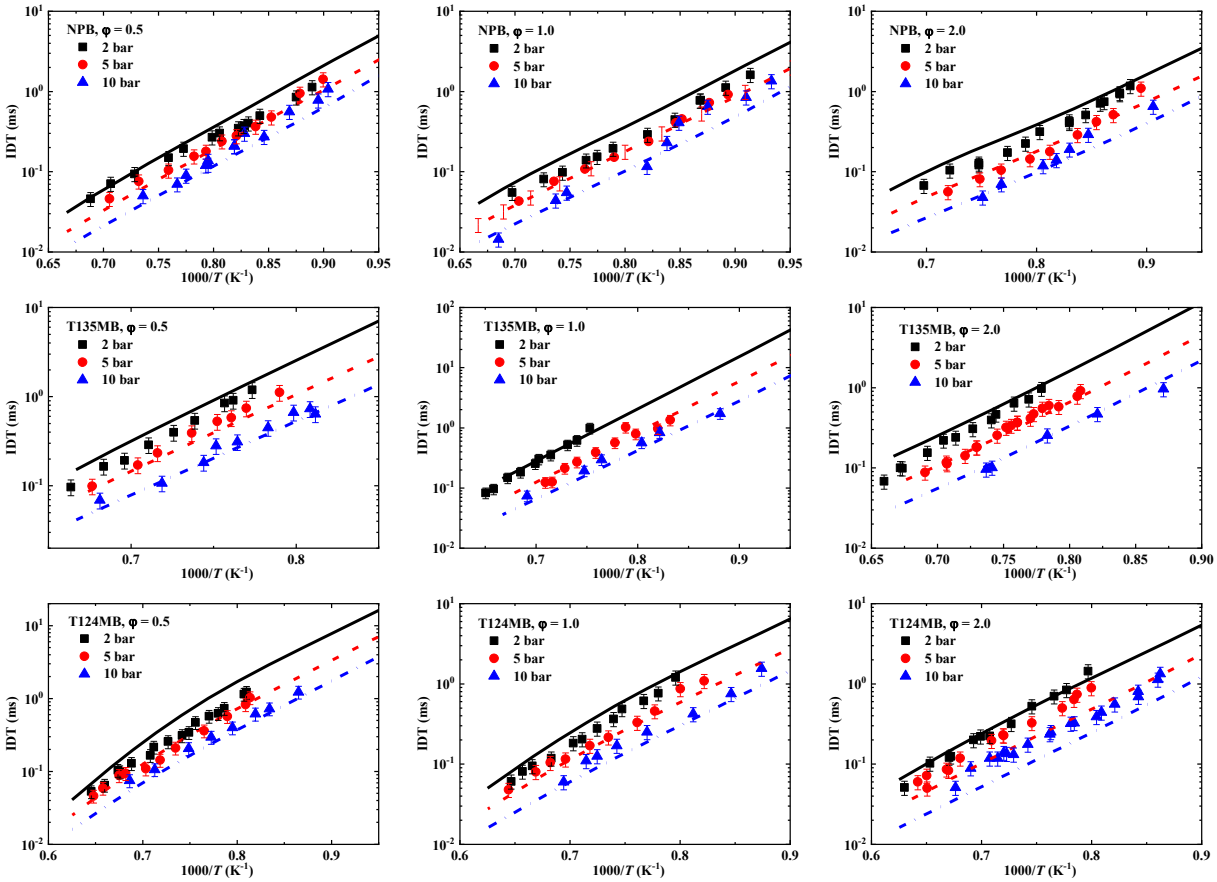

Fig. 3. Comparisons of predicted IDTs for NPB, T135MB, and T124MB with experimental measurements.

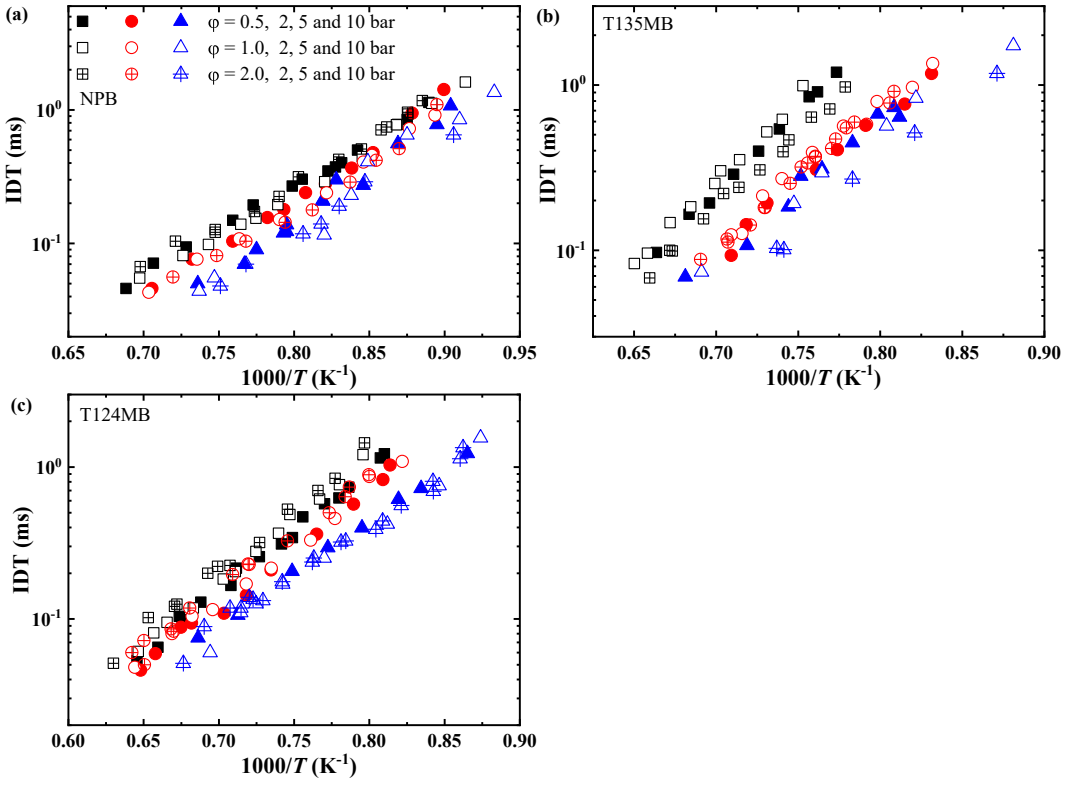

Fig. 4. Comparisons of measured IDTs for NPB, T135MB, and T124MB at 2, 5 and 10 bar with different equivalence ratios.

the universal gas constant. Fig. 5 shows the relationship between the ignition delay fitting curve and the experimental data. It is shown that linear relationship exists for all the three fuels. In addition, the activation energies of NPB, T135MB, and T124MB are 142279, 171698, and 145411 J mol^{-1}, respectively, which is also in good consistent with the observed overall reactivity from IDTs as shown in Fig. 2. Besides, it is also shown that the IDTs for the three fuels also satisfy a very good Arrhenius type relationship with the pressure, temperature, and equivalence ratios as the following equations (1) to (3). The fitted relationships between IDTs and different parameters for the three fuels should have a certain guiding significance for the selection of surrogate component and simulation and calculation of the related combustion properties in the combustion chamber.

$$\tau_{ign}(\mathrm{NPB}) = 6.04 \times 10^{-10} P^{-0.41} \varphi^{-0.11} exp(138021/RT) \quad (1)$$

$$\tau_{ign}(\mathrm{T135MB}) = 3.78 \times 10^{-10} P^{-0.71} \varphi^{-0.35} exp(163643/RT) \quad (2)$$

$$\tau_{ign}(\mathrm{T124MB}) = 2.09 \times 10^{-9} P^{-0.48} \varphi^{0.16} exp(139843/RT) \quad (3)$$

4.2. Sensitivity analysis

To further demonstrate the nature of chemical kinetics that affects the ignition characteristics of the three fuels, sensitivity analysis and reaction path analysis are carried out to reveal the dominant ignition chemistry. First, to identify key reactions affecting the ignition properties of the three C_9H_{12} fuels, brute-force sensitivity analysis [45] is performed using the detailed kinetic mechanism. Sensitivity analysis is conducted for IDTs assuming a closed homogeneous batch reactor at constant volume. The sensitivity coefficient is computed as $S_i = [\tau(2^*k_i)-\tau(k_i)]/\tau(k_i)$, where k_i is the rate constant of reaction i, $\tau(2^*k_i)$ is the IDT when the rate constant of reaction i is doubled, and $\tau(k_i)$ is the original predicted IDT. Consequently, a positive value of S_i means that the IDT becomes longer with an increasing rate constant of reaction i, and vice versa. The sensitivity coefficients are computed through a one-by-one procedure by changing the rate constant of one reaction at a time. Sensitivity analysis is performed for the three fuels at 5 bar and 1300 K with equivalence ratios of 0.5, 1.0, and 2.0. Fig. 6 shows the sensitivity analysis results for the three fuels at 5 bar and 1300 K with equivalence ratios of 1.0, while the results at the other conditions are provided in supplementary materials.

For NPB, it is shown that the initial decomposition reaction of NPB (denoted as PBZ) to the formation of benzyl and ethyl exhibits large negative sensitivity coefficient, while the three abstraction reactions by H and OH radicals demonstrate positive sensitivity coefficients. Specifically, it is shown that the reactions with negative sensitivity coefficients, i.e., accelerating the ignition delay time with large rate constants, are mostly related to the reactions with small C_0-C_4 molecules. The initial decomposition reaction of NPB to the formation of benzyl and ethyl radicals is one of the most important reactions affecting ignition because of the formed ethyl radical can quickly transform to ethylene and related small radicals, which are much more reactive than aromatic compounds/intermediates. It is also interesting to note that the two reaction channels of $C_6H_5CH_2$ with HO_2 to the formation of $C_6H_5CH_3 + O_2$ and $C_6H_5CH_2O + OH$ exhibit opposite effect on ignition delay times. The formation of toluene obviously increases the ignition delay time, while the formation of much more reactive benzaldehyde can decrease the ignition delay time. The abstraction reactions at the different sites in the propyl group also exhibit different effect from the observed sensitivity coefficients. The abstraction reactions at the primary site (PBZJA) and the secondary site near the aromatic ring (PBZJC) exhibit positive sensitivity coefficients, possibly due to the following β-scission reaction leading to the formation of benzyl or styrene species, which is less reactive. The abstraction reaction at the secondary site

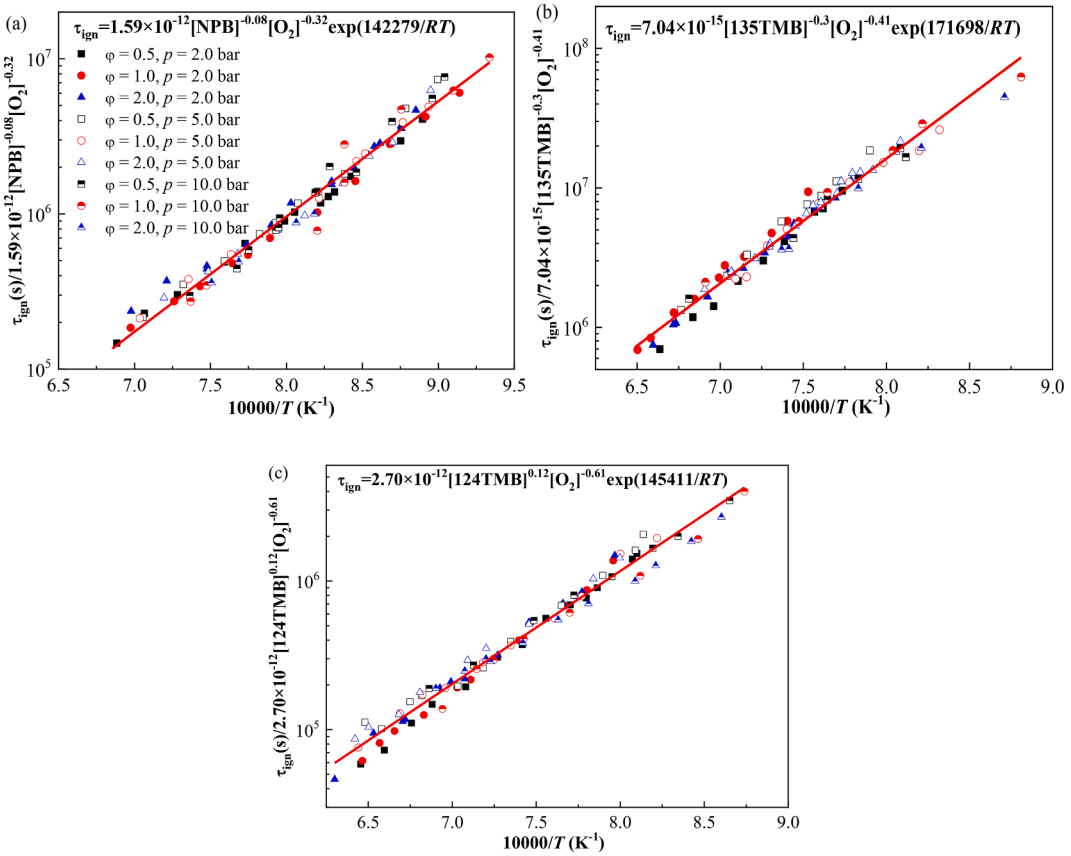

Fig. 5. Data fitting of IDTs of NPB, T135MB, and T124MB.

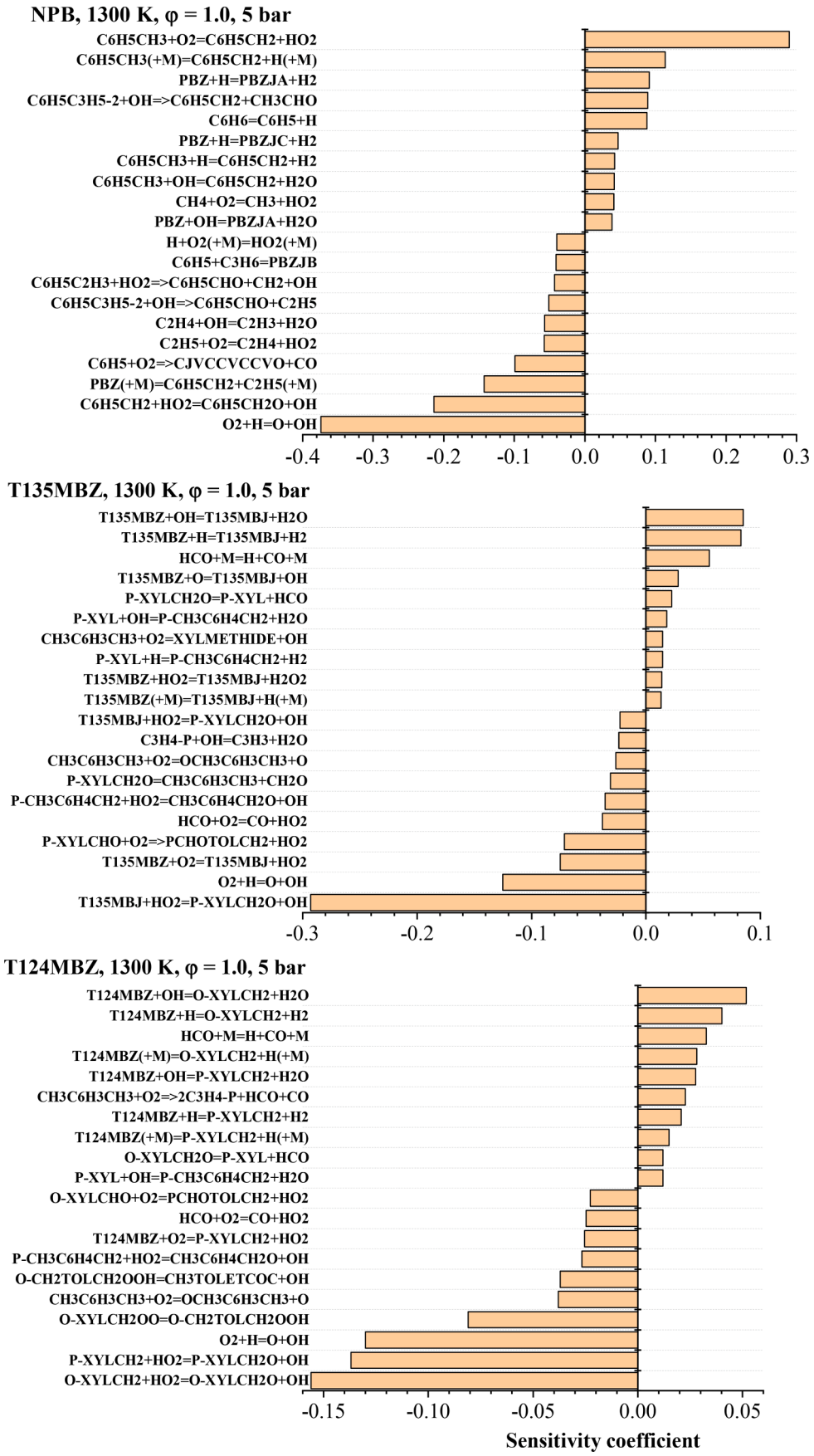

Fig. 6. Brute-force sensitivity coefficient for the three fuels at 1300 K and 5 bar with equivalence ratio of 1.0. The top ten reactions with negative and positive sensitivity coefficients are shown.

(PBZJB) close to the primary site is observed with a negative sensitivity coefficient due to the following reaction to the formation of phenyl and propene. To sum up, it is demonstrated that the initial reactions of NPB demonstrate very different effect on the ignition delay times due to the following reaction products. The following reactions related to toluene and benzene tend to show large effect on the IDT of NPB. The other reactions are mainly related to the important reactions of C_0-C_4 molecules, i.e., H_2, CH_4, and C_2H_4. The sensitivity analysis results of NPB are in good agreement with previous results [45].

For T124MB and T135MB (denoted as T124MBZ and T135MBZ in Fig. 6), it is demonstrated that the top sensitive reactions are mostly related to the fuel molecules and the following aromatic intermediates besides three reactions related to HCO and H, i.e., $O_2 + H = O + OH$, $HCO + M = H + CO + M$, and $HCO + O_2 = CO + HO_2$. Specifically speaking for T135MB, only one fuel radical (namely T135MBJ) can be formed sue to the symmetry structure, and it can be seen that the initial abstraction reactions by OH, H, and O radicals exhibit positive sensitivity coefficients on the IDTs, while the abstraction reactions by O_2 demonstrate negative sensitivity coefficients. Similar to the results of NPB, it is shown that the reaction of the fuel radical T135MBJ with HO_2 exhibits very large negative sensitivity coefficient. The other reactions are generally with small sensitivity coefficients. The global tendencies of the sensitivity analysis results of T124MB are generally in good accordance with that of T135MB, except that more fuels radicals can be formed from the initial abstraction reactions on T124MB due to the unsymmetric molecular structure. It can be seen that the abstraction reactions at these sites are both important with large sensitivity coefficients. Similarly, the reactions of the formed fuels radicals, i.e., O-$XYLCH_2$ and P-$XYLCH_2$ radicals, with HO_2 exhibit large effect on the IDTs with negative sensitivity coefficients. To sum up, for T124MB, the other important reactions are mostly related to the formed O-$XYLCH_2$ and P-$XYLCH_2$ radicals, while the other important reactions for T135MB are mostly related to the T135MBJ and subsequent formed P-$XYLCH_2O$ species.

Generally, from sensitivity analysis, it can be concluded that the most sensitive reactions for the three C_9H_{12} fuels share the very similar phenomena that the IDTs are critically affected by the initial abstraction or decomposition reactions of the fuel and the subsequent reactions from the formed radicals. But the specific species and related reactions are different because the formed fuel radicals are different, which is induced by the fuel molecular structure. It is also noted that the important reactions related to the base C_0-C_4 molecules revealed from sensitivity analysis of NPB are also slightly different compared with T124MB and T135MB. Specifically, due to the propyl group in NPB, the reactions related to C_2H_4, C_2H_5 and CH_3 also show large effect on the IDTs of NPB. However, reactions related to the base C_0-C_4 molecules affecting the IDTs of T124MB and T135MB are nearly the following reactions related to HCO and H, i.e., $O_2 + H = O + OH$, $HCO + M = H + CO + M$, and $HCO + O_2 = CO + HO_2$. Sensitivity analysis at the other equivalence ratios, i.e., 0.5 and 2.0, also reveals the same conclusions.

4.3. Reaction path analysis

To further demonstrate the differences of the detailed mechanisms of the three C_9H_{12} fuels, reaction path analysis is carried out using rate-of-production (ROP) analysis during the ignition simulation processes. Figs. 7-9 show the ROP analysis results for NPB, T135MB, and T124MB at $\varphi = 1.0$ in air at 1300 K and 5 bar with 20% fuel consumption, respectively. For NPB, the major initial reactions are the decomposition reaction to ethyl and benzyl radicals and the abstraction reactions at the propyl group. The results are also in good accordance with the bond energies at the reaction sites. Generally, the C–C dissociation energy at the propyl group is lower about 3–5 kcal/mol compared with the C–C bond linking the alkyl and phenyl group [46]. Due to the large consumption of NPB from the decomposition reaction to ethyl and phenyl radicals, the reactions related to phenyl and toluene exhibit large effect on the IDTs as revealed from sensitivity analysis. From Fig. 7, three major reaction path related to phenyl radical is observed. The formation of toluene, ethylbenzene, and large aromatic compound ($C_{14}H_{14}$) are all important. The following reactions related to the three fuel radicals from abstraction reactions at the propyl group are mostly β-scission reactions. It can be seen that styrene, allyl benzene, prop-1-en-1-ylbenzene represent the major products, which can follow similar reactions based on ethylene and propene to the formation of benzaldehyde, phenyl and related products. Further, large aromatic compounds including indene and $C_{14}H_{14}$ related to soot are also observed from ROP analysis. Besides these aromatic compounds, it is shown that the small molecules including ethylene, ethyl, and propene are formed through

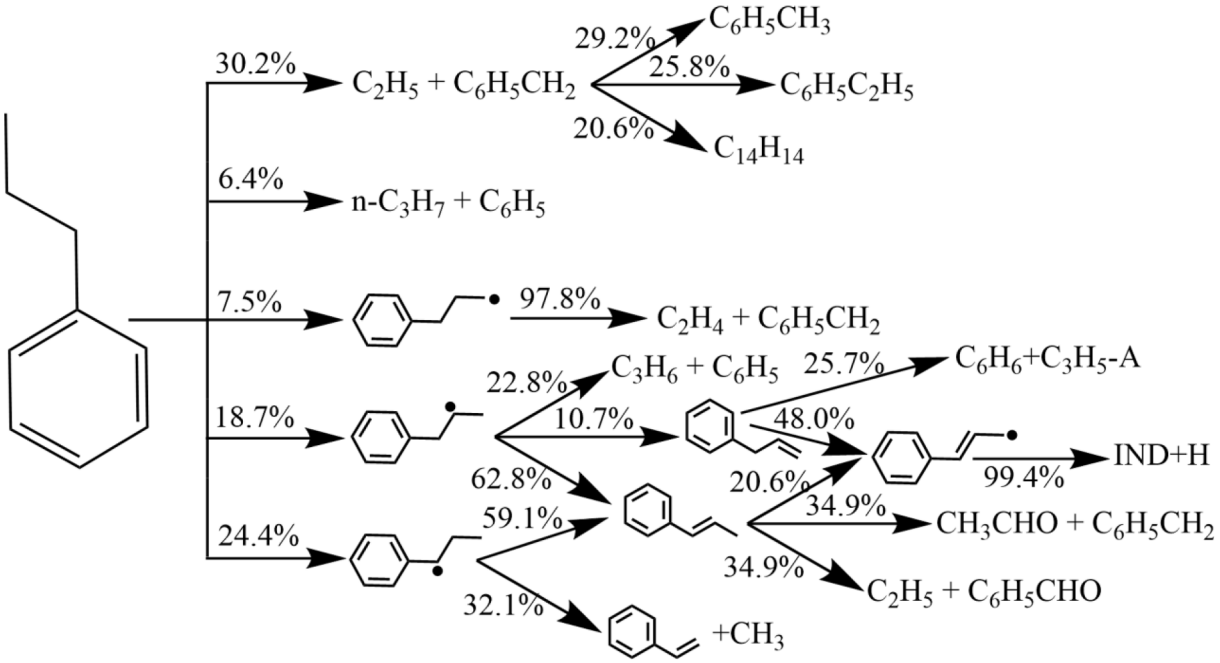

Fig. 7. ROP analyses for NPB at $\varphi = 1.0$ in air at 1300 K and 5 bar with 20% fuel consumption during ignition process.

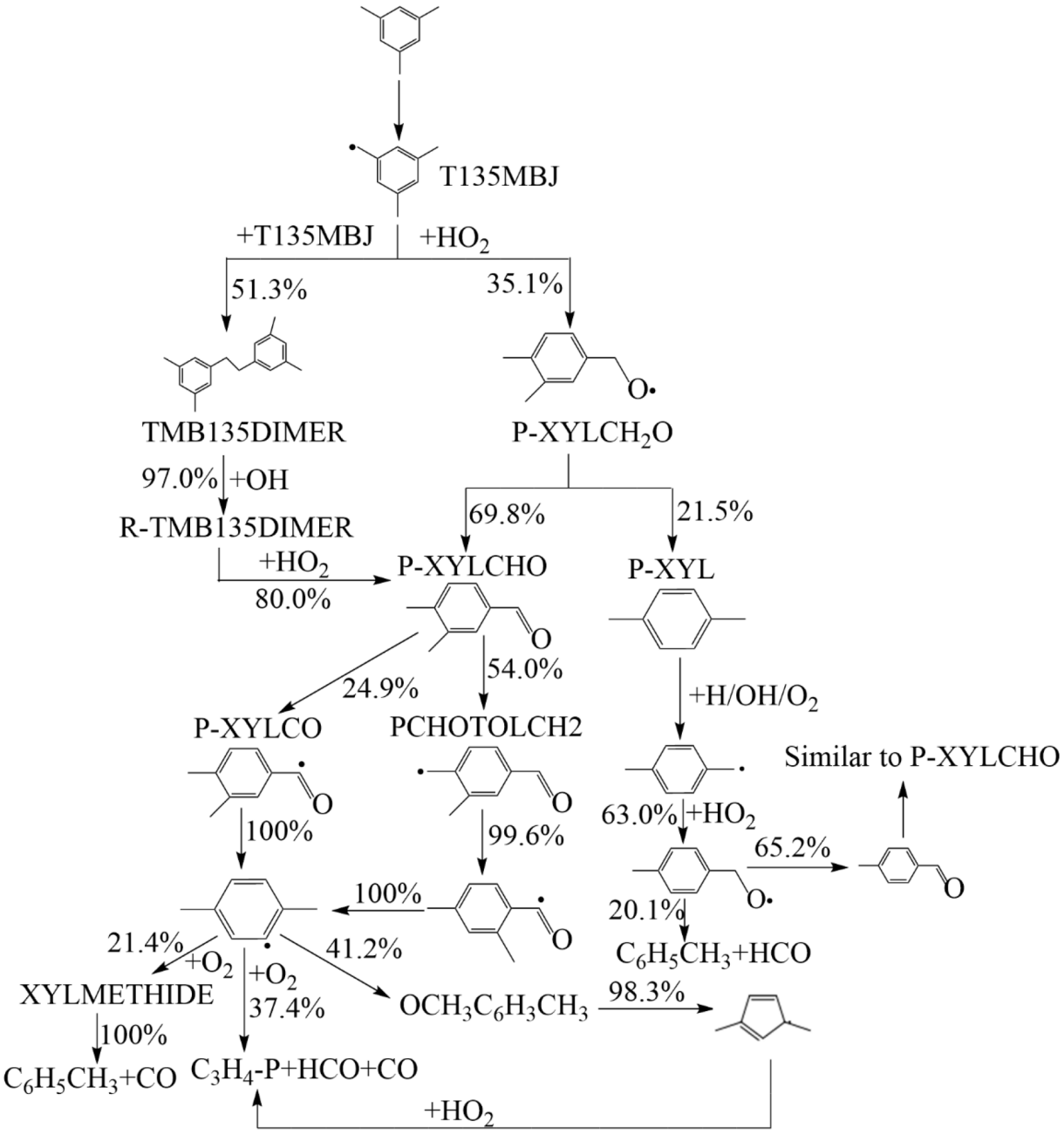

Fig. 8. ROP analyses for T135MBZ at φ = 1.0 in air at 1300 K and 5 bar with 20% fuel consumption during ignition process.

the β-scission reactions, which also show large effect on IDTs of NPB. This is also revealed from sensitivity analysis results as shown in Fig. 6. The overall reaction path for NPB is also in good agreement with previous studies [11,12,45,47].

For T135MB and T124MB, the major reaction path demonstrates large differences compared with NPB due to the fuel structure effect as shown in Figs. 8 and 9. Specifically, the initial reactions of T135MB are mainly related to the abstraction reactions due to the direct decomposition of C–C bond linking the methyl and benzyl radicals is difficult. The formed T135MBJ radical are mainly through two paths: the recombination reaction of T135MBJ itself and the reaction with HO_2 radical to the formation of P-XYLCH$_2$O. It is worth noting that the recombination reaction of T135MBJ contributes half percent consumption of T135MBJ. The following reaction of TMB135DIMER are lumped, and the reaction with OH radical completely controls its consumption to the formation of corresponding radical, which further reacts with HO_2 to the formation of P-XYLCHO. It is noted that the P-XYLCHO is also the major product of the P-XYLCH$_2$O, indicating that the P-XYLCHO is an important intermediate during the oxidation of T135MB. A certain number of P-XYL is also formed via P-XYLCH$_2$O, and the following reaction sequences are very similar to toluene, i.e., the abstraction reactions at the methyl site and then following with HO_2 to the formation of $CH_3C_6H_5CH_2O$ species. Following oxidation of P-XYLCHO is mainly through the abstraction reactions at the aldehyde group and the methyl group, which lead to the formation of P-XYL radical at the benzene group ($CH_3C_6H_3CH_3$). Finally, it is shown that these large intermediates are toward to the formation of propyne as the major small fuels through the reaction $CH_3C_6H_3CH_3 + O_2 = 2C_3H_4\text{-P} + HCO + CO$. Consequently, this also explains why the reaction $C_3H_4\text{-P} + OH = C_2H_3 + H_2O$ demonstrates large effect on the IDTs of T135MBZ as shown from sensitivity analysis. Compared with the results from NPB, toluene is only formed at a small level due to the long reaction path.

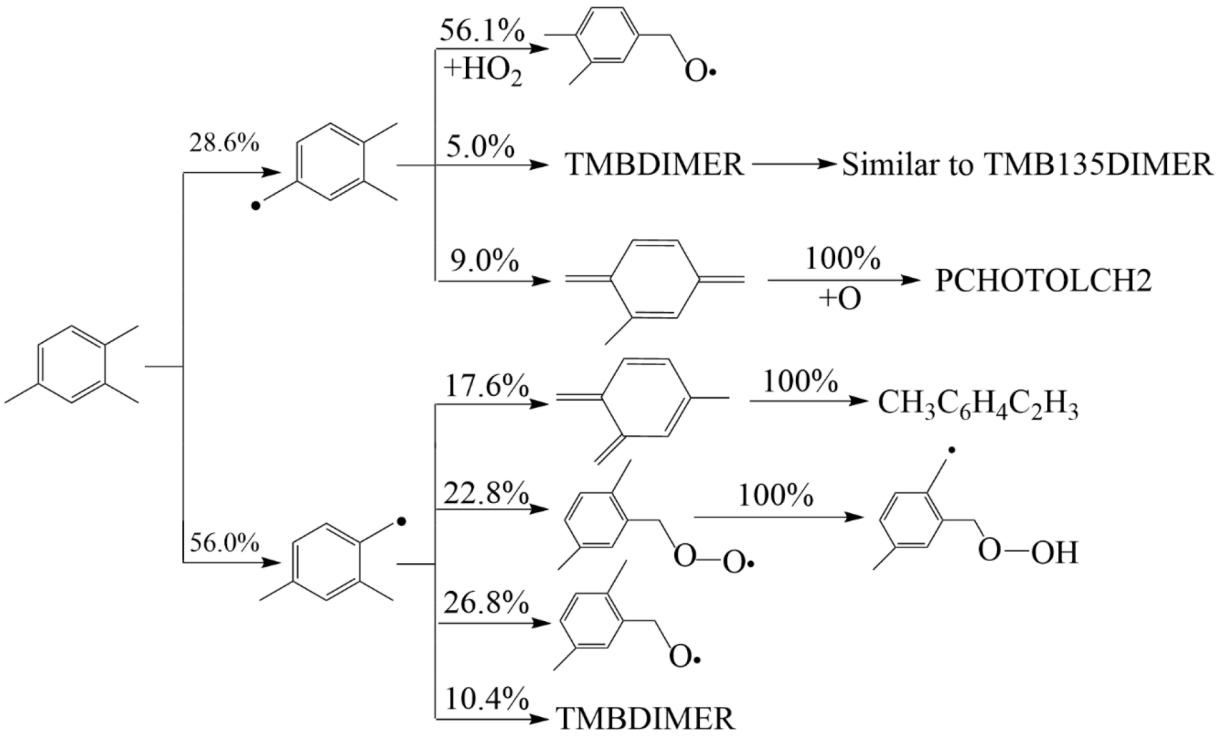

Fig. 9. ROP analyses for T124MBZ at φ = 1.0 in air at 1300 K and 5 bar with 20% fuel consumption during ignition process.

Due to the structure similar between T124MB and T135MB, the major reaction path from ROP analysis of T124MB tends to be simple as shown from Fig. 9 because the two fuels share some same intermediates. From Fig. 9, the major initial reactions are also the abstraction reactions, which is similar to T135MB. However, it is worth noting that the three fuel radicals at the three methyl groups are lumped as two fuel radicals as shown in Fig. 9. The formed two fuel radicals also go through recombination reactions to the formation of TMB135DIMER and TMBDIMER, which undergo the similar reactions as shown in Fig. 8. The following reaction paths related to the intermediates including P-XYL-CH_2O and PCHOTOLCH2 can be found in Fig. 8. However, compared with T135MB, it can be seen that the formed P-XYLCH_2O radical tends to be larger during the oxidation of T124MB, while a large amount of T135MBJ radical tends to the formation of large TMB135DIMER. The more reactivity of P-XYLCH_2O radical compared with the TMB135DIMER is probably the major reason that explains why the T124MB shows shorter IDTs compared with T135MB. However, as the equivalence ratio increases, the recombination reactions of the formed fuel radicals from T124MB tend to also contribute more to the formation of TMBDIMER, which makes the IDTs between T124MB and T135MB become closer. To sum up, reaction path analysis results indicates that large differences can be observed between NPB and T124MB/T135MB. NPB generally undergoes traditional high-temperature reaction path involving the reaction classes, i.e., abstraction reaction and β-scission reaction classes. Benzene and toluene are major intermediates during the oxidation of NPB. For T135MB and T124MB, it is shown that the recombination reactions of the fuel radicals play an important role in the mechanism development, and the major intermediates are related to the formed aromatic aldehyde and ketone compounds.

5. Conclusions

This work reports a comparative experimental and kinetic modeling study of the high-temperature ignition of three C_9H_{12} fuels including n-propylbenzene (NPB), 1,3,5-trimethylbenzene (T135MB), and 1,2,4-trimethylbenzene (T124MB). New ignition delay times (IDTs) are measured in a high-pressure shock tube (HPST). A universal mechanism is developed based on the previous kinetic models to simulate the experimental results. Major conclusions are summarized as follows:

(1) The measured IDTs indicate that the overall reactivity of the three C_9H_{12} fuels exhibit the following tendency with NPB > T124MB > T135MB. But the relative reactivity of T124MB and T135MB tends to become close to each other as the equivalence ratio increases to 2.0.
(2) The measured IDTs of the three fuels are all affected by the pressure and temperature significantly, but the effect of equivalence ratio is very minor. The IDTs are fitted into Arrhenius type relationships with pressure, temperature, and equivalence ratio.
(3) Sensitivity analysis shows that both the initial abstraction or direct decomposition reactions and the important base C_0-C_4 molecule involved reactions play critical role for NPB, while the dominant reactions of T135MB and T124MB are mostly related to the initial abstraction reactions and the following reactions related to the fuel radicals.
(4) ROP analysis results reveal that the initial reaction path of NPB is mainly through abstraction and decomposition reactions directly, and the following reactions of fuel radicals mainly undergo β-scission reactions, while the initial reaction path of T124MB and T135MB are completely dominant by abstraction reactions (under the considered conditions) and the following fuel radical reactions are more complicated.
(5) The present mechanism could reasonably predict the measured IDTs, and explain the observed different reactivity of the three fuels. However, further improvement of the detailed mechanisms including comprehensive consideration the initial reaction of T124MB and the reaction path related to the formed dimers are required to get a better understanding of the combustion chemistry of the three fuels. In general, the present results and comparisons provide valuable information to get insight into the combustion kinetic of these fuels which are potential surrogate fuel constituents for real fuels.

Declaration of Competing Interest

The authors declare that they have no known competing financial interests or personal relationships that could have appeared to influence the work reported in this paper.

Acknowledgments

J. Liang acknowledges funding from the Natural Science Foundation of China (12172335), Research Project Supported by Shanxi Scholarship Council of China (No. 2020-115; Fei Li acknowledges funding from the Graduate Innovation Project of Shanxi Province (2021Y654); Q.-D. Wang acknowledges financial support by the Natural Science Foundation of China (U2133215) and Fundamental Research Funds for the Central Universities of China (No. 2020ZDPYMS05).

References

[1] Sarathy SM, Farooq A, Kalghatgi GT. Recent progress in gasoline surrogate fuels. Prog Energy Combust Sci 2018;65:67–108.
[2] Battin-Leclerc F. Detailed chemical kinetic models for the low-temperature combustion of hydrocarbons with application to gasoline and diesel fuel surrogates. Prog Energy Combust Sci 2008;34(4):440–98.
[3] Yang Z-Y, Zeng P, Wang B-Y, Jia W, Xia Z-X, Liang J, et al. Ignition characteristics of an alternative kerosene from direct coal liquefaction and its blends with conventional RP-3 jet fuel. Fuel 2021;291:120258.
[4] Das DD, John PCS, McEnally CS, Kim S, Pfefferle LD. Measuring and predicting sooting tendencies of oxygenates, alkanes, alkenes, cycloalkanes, and aromatics on a unified scale. Combust Flame 2018;190:349–64.
[5] Wu Z, Mao Y, Raza M, Zhu J, Feng Y, Wang S, et al. Surrogate fuels for RP-3 kerosene formulated by emulating molecular structures, functional groups, physical and chemical properties. Combust Flame 2019;208:388–401.
[6] Jin Z-H, Chen J-T, Song S-B, Tian D-X, Yang J-Z, Tian Z-Y. Pyrolysis study of a three-component surrogate jet fuel. Combust Flame 2021;226:190–9.
[7] Xu JQ, Guo JJ, Liu AK, Wang JL, Tan NX, Li XY. Construction of Autoignition Mechanisms for the Combustion of RP-3 Surrogate Fuel and Kinetics Simulation. Acta Phys Chim Sin 2015;31(4):643–52.
[8] Yan YW, Liu YC, Fang W, Liu YP, Li JH. A simplified chemical reaction mechanism for two-component RP-3 kerosene surrogate fuel and its verification. Fuel 2018;227:127–34.
[9] Honnet S, Seshadri K, Niemann U, Peters N. A surrogate fuel for kerosene. Proc Combust Inst 2009;32(1):485–92.
[10] Dooley S, Won SH, Heyne J, Farouk TI, Ju Y, Dryer FL, et al. The experimental evaluation of a methodology for surrogate fuel formulation to emulate gas phase combustion kinetic phenomena. Combust Flame 2012;159(4):1444–66.
[11] Liu Y-X, Wang B-Y, Weng J-J, Yu D, Richter S, Kick T, et al. A wide-range experimental and modeling study of oxidation and combustion of n-propylbenzene. Combust Flame 2018;191:53–65.
[12] Yuan WH, Li YY, Dagaut P, Wang YZ, Wang ZD, Qi F. A comprehensive experimental and kinetic modeling study of n-propylbenzene combustion. Combust Flame 2017;186:178–92.
[13] Mehl M, Herbinet O, Dirrenberger P, Bounaceur R, Glaude P-A, Battin-Leclerc F, et al. Experimental and modeling study of burning velocities for alkyl aromatic components relevant to diesel fuels. Proc Combust Inst 2015;35(1):341–8.
[14] Ji CS, Dames E, Wang H, Egolfopoulos FN. Propagation and extinction of benzene and alkylated benzene flames. Combust Flame 2012;159(3):1070–81.
[15] Conturso M, Sirignano M, D'Anna A. Effect of C9H12 alkylbenzenes on particle formation in diffusion flames: An experimental study. Fuel 2017;191:204–11.
[16] Tian D-X, Liu Y-X, Wang B-Y, Cao C-C, Liu Z-K, Zhai Y-T, et al. Pyrolysis study of iso-propylbenzene with photoionization and molecular beam mass spectrometry. Combust Flame 2019;209:313–21.
[17] Roubaud A, Minetti R, Sochet LR. Oxidation and combustion of low alkylbenzenes at high pressure: Comparative reactivity and auto-ignition. Combust Flame 2000;121(3):535–41.
[18] Liu Y, Tang CL, Wu YT, Yang M, Huang ZH. Low temperature ignition delay times measurements of 1,3,5-trimethylbenzene by rapid compression machine. Fuel 2019;241:637–45.
[19] Rao F, Li B, Li P, Zhang CH, Li XY. Shock-Tube Study of the Ignition of Gas-Phase 1,3,5-Trimethylbenzene in Air. Energy Fuels 2014;28(11):6707–13.
[20] Hui X, Das AK, Kumar K, Sung CJ, Dooley S, Dryer FL. Laminar flame speeds and extinction stretch rates of selected aromatic hydrocarbons. Fuel 2012;97:695–702.
[21] Hui X, Sung CJ. Laminar flame speeds of transportation-relevant hydrocarbons and jet fuels at elevated temperatures and pressures. Fuel 2013;109:191–200.
[22] Liu YX, Tian ZY. Oxidation chemistry of four C9H12 isomeric transportation fuels: Experimental and modeling studies. Combust Flame 2019;205:165–79.
[23] Panigrahy S, Liang J, Ghosh MK, Wang Q-D, Zuo Z, Nagaraja S, et al. An experimental and detailed kinetic modeling study of the pyrolysis and oxidation of allene and propyne over a wide range of conditions. Combust Flame 2021;233:111578.
[24] Morley C. Gaseq: a chemical equilibrium program for Windows. 0.79 ed.; 2005.
[25] Petersen EL, Rickard MJA, Crofton MW, Abbey ED, Traum MJ, Kalitan DM. A facility for gas- and condensed-phase measurements behind shock waves. Measurement Science Technology 2005;16(9):1716–29.
[26] Baigmohammadi M, Patel V, Nagaraja S, Ramalingam A, Martinez S, Panigrahy S, et al. Comprehensive Experimental and Simulation Study of the Ignition Delay Time Characteristics of Binary Blended Methane, Ethane, and Ethylene over a Wide Range of Temperature, Pressure, Equivalence Ratio, and Dilution. Energy Fuels 2020;34(7):8808–23.
[27] Baigmohammadi M, Patel V, Martinez S, Panigrahy S, Ramalingam A, Burke U, et al. A comprehensive experimental and simulation study of ignition delay time characteristics of single fuel C1–C2 hydrocarbons over a wide range of temperatures, pressures, equivalence ratios, and dilutions. Energy Fuels 2020;34(3):3755–71.
[28] Panigrahy S, Liang J, Nagaraja SS, Zuo Z, Kim G, Dong S, et al. A comprehensive experimental and improved kinetic modeling study on the pyrolysis and oxidation of propyne. Proc Combust Inst 2021;38(1):479–88.
[29] Guzman J, Kukkadapu G, Brezinsky K, Westbrook C. Experimental and modeling study of the pyrolysis and oxidation of an iso-paraffinic alcohol-to-jet fuel. Combust Flame 2019;201:57–64.
[30] Mulvihill CR, Mathieu O, Petersen EL. H_2O time histories in the H_2-NO_2 system for validation of NOx hydrocarbon kinetics mechanisms. Int J Chem Kinet 2019;51(9):669–78.
[31] Wang Q-D, Panigrahy S, Yang S, Martinez S, Liang J, Curran HJ. Development of Multipurpose Skeletal Core Combustion Chemical Kinetic Mechanisms. Energy Fuels 2021;35(8):6921–7.
[32] Ramalingam A, Panigrahy S, Fenard Y, Curran H, Heufer KA. A chemical kinetic perspective on the low-temperature oxidation of propane/propene mixtures through experiments and kinetic analyses. Combust Flame 2021;223:361–75.
[33] Pelucchi M, Cai L, Pejpichestakul W, Tripathi R, Wagnon S, Zhang K, et al. Computational Chemistry Consortium: Surrogate Fuel Mechanism Development, Pollutants Sub-Mechanisms and Components Library. SAE Technical Paper 2019–24-0020..
[34] Nagaraja SS, Liang J, Dong S, Panigrahy S, Sahu A, Kukkadapu G, et al. A hierarchical single-pulse shock tube pyrolysis study of C_2–C_6 1-alkenes. Combust Flame 2020;219:456–66.
[35] Nagaraja SS, Sahu AB, Panigrahy S, Curran HJ. A fundamental study on the pyrolysis of hydrocarbons. Combust Flame 2021;233:111579.
[36] Wang H, Dames E, Sirjean B, Sheen DA, Tangko R, Violi A, et al. JetSurF II: a high temperature chemical kinetic model of n-alkane (up to n-dodecane), cyclohexane, and methyl-, ethyl-, n-propyl and n-butyl-cyclohexane oxidation at high temperatures, http://web.stanford.edu/group/haiwanglab/JetSurF/JetSurF2.0/; 2017. 2017].
[37] Kukkadapu G, Kang D, Wagnon SW, Zhang K, Mehl M, Monge-Palacios M, et al. Kinetic modeling study of surrogate components for gasoline, jet and diesel fuels: C7–C11 methylated aromatics. Proc Combust Inst 2019;37(1):521–9.
[38] Goodwin DG, Speth RL, Moffat HK, Weber BW. Cantera: An Object-oriented Software Toolkit for Chemical Kinetics, Thermodynamics, and Transport Processes. Version 2.4.0 ed.; 2018.
[39] Davidson DF, Hanson RK. Recent advances in shock tube/laser diagnostic methods for improved chemical kinetics measurements. Shock Waves 2009;19(4):271–83.
[40] Pang GA, Davidson DF, Hanson RK. Experimental study and modeling of shock tube ignition delay times for hydrogen-oxygen-argon mixtures at low temperatures. Proc Combust Inst 2009;32(1):181–8.
[41] Sung CJ, Curran HJ. Using rapid compression machines for chemical kinetics studies. Prog Energy Combust Sci 2014;44:1–18.
[42] Darcy D, Tobin CJ, Yasunaga K, Simmie JM, Würmel J, Metcalfe WK, et al. A high pressure shock tube study of n-propylbenzene oxidation and its comparison with n-butylbenzene. Combust Flame 2012;159(7):2219–32.
[43] Diévart P, Kim HH, Won SH, Ju Y, Dryer FL, Dooley S, et al. The combustion properties of 1,3,5-trimethylbenzene and a kinetic model. Fuel 2013;109:125–36.
[44] Chen BH, Liu JZ, Yao F, He Y, Yang WJ. Ignition delay characteristics of RP-3 under ultra-low pressure (0.01-0.1 MPa). Combust Flame 2019;210:126–33.
[45] Wang Q-D, Fang Y-M, Wang F, Li X-Y. Systematic analysis and reduction of combustion mechanisms for ignition of multi-component kerosene surrogate. Proc Combust Inst 2013;34(1):187–95.
[46] Luo Y-R. Handbook of bond dissociation energies in organic compounds. CRC Press; 2002.
[47] Darcy D, Mehl M, Simmie JM, Würmel J, Metcalfe WK, Westbrook CK, et al. An experimental and modeling study of the shock tube ignition of a mixture of n-heptane and n-propylbenzene as a surrogate for a large alkyl benzene. Proc Combust Inst 2013;34(1):411–8.